Available online at www.sciencedirect.com
SCIENCE DIRECT®
Organic Electronics 5 (2004) 271–281
Organic Electronics
www.elsevier.com/locate/orgel

Role of LiF in polymer light-emitting diodes with LiF-modified cathodes

Y.D. Jin [a], X.B. Ding [a], J. Reynaert [a], V.I. Arkhipov [a], G. Borghs [a], P.L. Heremans [a], M. Van der Auweraer [b,*]

[a] *Interuniversity Micro-Electronics Center (IMEC), Kapeldreef 75, Leuven B 3001, Belgium*
[b] *Department of Chemistry, Laboratory for Molecular Dynamics and Spectroscopy, Katholieke Universiteit Leuven (K.U. Leuven), Celestijnenlaan 200 F, Leuven B 3001, Belgium*

Received 15 January 2004; received in revised form 9 July 2004; accepted 13 August 2004
Available online 17 September 2004

Abstract

We report on high-efficiency polymer light-emitting diodes (PLEDs) based on poly [2-methoxy-5-(3′,7′-dimethyloctyloxyl)]-1,4-phenylene vinylene (OC1C10) with LiF-modified cathodes. Devices with different cathodes are made and characterized by the electroabsorption technique to measure their built-in voltage. Devices with a LiF/Al bilayer cathode or a LiF:Al composite cathode, all show significantly improved performance as compared to those with bare Al cathodes. The improvement is correlated with enhanced electron injection due to a decrease of the electron injection barrier, which is also indicated by the electroabsorption measurements. The same effect is also observed with LiF(0.6 nm)/Mg cathodes. However, inserting the same LiF thin film between Ag and OC1C10 does not improve the device performance. Cathodes composed of ultra-thin films of LiF(0.6 nm)/Al(1 nm) or LiF:Al(2 nm) covered by Ag (100 nm) show the same performance as LiF(0.6 nm)/Al bilayer cathode or a LiF:Al composite cathode, indicating that the enhancement is specific to LiF and Al. Our experiments can be explained by assuming that Li-ions can dissociate from LiF and diffuse into the OC1C10 layer, leading to an n-type zone close to the polymer/cathode interface. This n-doped layer at the interface facilitates electron injection at the cathode/polymer interface and eventually leads to the formation of an Ohmic contact.

PACS: 72.80.Le; 73.61.Ph
Keywords: Polymer light-emitting diodes; LiF; Electron injection; Electroabsorption; Built-in potential; n-Type doping

* Corresponding author. Tel.: +32 16 327 496; fax: +32 16 327 990.
E-mail address: mark.vanderauweraer@chem.kuleuven.ac.be (M. Van der Auweraer).

1566-1199/$ - see front matter
doi:10.1016/j.orgel.2004.08.001

1. Introduction

The nature of the interface between active light-emitting polymers and metal electrodes is of paramount importance for the efficiency and lifetime of polymer light emitting diodes (PLEDs) [1,2]. The polymer/metal interface is often treated in a rigid band structure model in which the charge injection efficiency is determined by the barrier height. In devices where the anodic barrier is low, a major improvement in device efficiency and lifetime is expected by reducing the cathodic barrier. Therefore low work function metals such as calcium are commonly used as cathodes. However, calcium's reactivity creates reliability problems for handling during both fabrication and encapsulation. It has been shown that the use of an air-stable bilayer LiF/Al cathode can increase the electron injecting in the devices based on organic molecular semiconductors, such as Alq_3 [3,4], or polymeric semiconductors such as a polyarylene derivative [5], polyfluorenes (PFO) [6,7], and poly [2-methoxy-5-(2-ethylhexoxy)-1,4-phenylenevinylene] (MEH-PPV) [8,9]. Different mechanisms have been proposed in the literature to explain the role of LiF for the improvement on electron injection. They include tunnelling [3], decrease of the surface potential due to polarization of LiF under the Al surface [9], disproportionation and dissociation of LiF [8], and protection of the polymer from damage during Al deposition [10]. However, the dominant mechanism for the improved electron injection in polymer LEDs in the presence of LiF remains a subject of debate.

In this paper, we carry out a set of systematic experiments to study the role of LiF in such LiF-modified cathodes for PLEDs. Devices with different cathodes are tested and electroabsorption measurements are done to characterize thebuilt-in voltage inside these devices. Poly [2-methoxy-5-(3′,7′-dimethyloctyloxyl)]-1,4-phenylene vinylene (OC1C10 in short) [11], an archetype light-emitting polymer, is used as the active material in the devices. We first examine the effect of inserting LiF thin film between OC1C10 and different metals, such as Al, Mg and Ag. We then investigated the dependence of device efficiency on LiF thickness in the LiF/Al cathodes. Furthermore, we compare LiF/Al and LiF:Al composite, both covered by thick Al layers, with LiF/Al/Ag and LiF:Al/Ag electrodes, both with ultrathin LiF/Al bilayer or LiF:Al composite films, in terms of PLED efficiency and built-in voltage. Our results lead to formulate a mechanism, which explains the observed role of LiF.

Besides current voltage plots and luminescence efficiency also the electroabsorption [11–13] was determined. This technique is based on the increase or decrease of the absorbance of a sample in the presence of an electric field. In electroabsorption experiments this electric field has a static and a dynamic component (E_{DC} and E_{AC}).

$$\Delta A(\omega) \propto \chi_2(\omega,0)(E_{DC}+E_{AC}) + \chi_3(\omega,0,0)(E_{DC}+E_{AC})^2. \quad (1)$$

For a centrosymmetric sample the χ_2 term may be neglected compared to the χ_3 term [14,15]. This leads to an electroabsorption signal ΔA proportional to the square of the total applied field.

$$\Delta A(\omega) \propto \chi_3(\omega,0,0)(E_{DC}+E_{AC})^2 = \chi_3(\omega,0,0)(E_{DC}^2+2E_{DC}E_{AC}+E_{AC}^2). \quad (2)$$

The component of ΔA which varies with the same frequency as the applied AC field $\chi_3(\omega,0,0)$-$E_D E_{AC}$ will disappear in the absence of the DC field. In the presence of an internal electric field in the sample (due to space charges or Schottky barriers) an external bias voltage opposite and equal to the built-in potential, has to be applied to arrive at a (DC) field free sample bulk. In this way the built-in potential difference over the sample can be determined.

2. Experiments

The details of substrate preparation are described in [16]. All devices had a 25-nm layer of poly-(3,4)-ethylenedioxythiophene-polystyrenesulfonate (PEDOT-PSS) film as a hole-injection layer. OC1C10 material was synthesized by Gilch route, and used as received [17]. OC1C10 was dissolved in chlorobenzene and spin coated on the PEDOT-PSS layer to form a 110 ± 10 nm film at room temperature. Top metal contacts were

consecutively thermally evaporated in a UHV set-up with deposition rates of 0.1 Å/s for LiF and 1.5–3.5 Å/s for metals at a base pressure of 5×10^{-9} Torr. LiF and Al composite electrodes were realized by a co-deposition from separate sources. The LiF content in such composite is ~3 wt%. We term the electrodes composed of LiF/Al bilayer as "LiF/Al" where the LiF thickness is 0.6 nm unless it is otherwise specified. The electrodes composed of LiF and Al composite is termed as "LiF:Al". Except for spin casting of PEDOT-PSS, fabrication and characterization of the devices were done in a nitrogen box.

Current–luminance–voltage characteristics were measured using a HP 4145B parameter analyzer coupled to a calibrated photodiode (Newport 8320). The efficiency and luminance of the devices were measured by a calibrated silicon photodetector placed close to the bottom of the substrate. The luminance (cd/m^2) of PLEDs was converted from the radiant power by assuming an angular distribution of Lambertian emission. It is worth noting that the efficiencies reported here are measured for the light emitted in the viewing hemisphere only. Therefore, the light output measured with an integrating sphere could be larger than the value reported in the present work [18,19]. Thus, all the quantum efficiencies reported here represent the lower limits on the "true" η_{ext} and a fortiori on the internal quantum efficiency (η_{int}). As all devices had a similar construction differences in the measured device performance will reflect changes in the internal quantum efficiency (η_{int}).

For the electroabsorption experiments, excitation occurred at 590 nm (2.1 eV) which was slightly to the red of the zero–zero transition of the lowest absorption band. Taking into account the existing electron phonon coupling this energy corresponds to the bandgap energy of OC1C10. The experiments were performed by applying a 2 V (peak to peak) oscillating voltage with a frequency of 720 Hz to the sample, generated by HP116A function generator. The component of ΔA (Change of the Absorption) which varies periodically with the applied oscillating voltage was isolated using a lock in amplifier. The experiments were executed at 77 K to obtain a better signal to noise ratio related (besides other effects) to the narrowing of the absorption bands at 77 K [20].

3. Results and discussions

Fig. 1 compares the current–voltage (I–V) and luminance–voltage (B–V) characteristics of two typical devices. Device (I) has a bare Al cathode (50 nm) and device (II) has a LiF(0.6 nm)/Al(50 nm) bilayer cathode. While the current density of device (II) corresponds to that obtained in the literature for similar devices [11,21] or devices with a low molecular active layer [22] the current density observed for device (I) is about an order of magnitude lower. Furthermore device (II) shows a luminance which is several orders of magnitude larger than that observed for device (I). Taking into account that PPV is essentially a hole transporting material, especially when using an aluminum cathode, this would indicate improved electron injection in device (II). Luminance of 100, 1000 and 10 000 Cd/m^2 can be achieved in device (II) at 3.2 V, 4.9 V and 8.2 V, respectively. The external forward EL quantum yield (η_{el}, photons emitted into the viewing hemisphere per charge flow) of device (II) was $2.0 \pm 0.2\%$, at an applied bias of -10 V which is 10 times higher than η_{el} of device (I) ($0.22 \pm 0.02\%$) at an applied bias of -10 V. The performance of device (II) is comparable to the performance of OC1C10-based devices

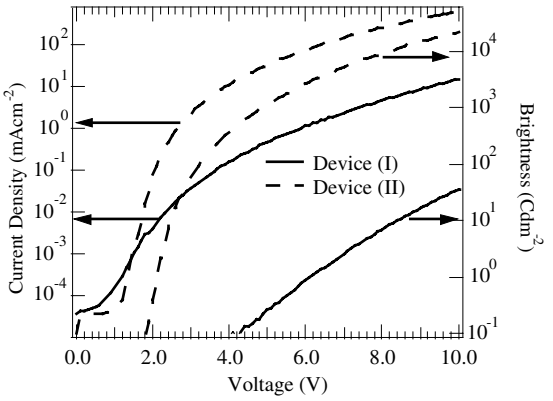

Fig. 1. I–V and luminance–voltage characteristics of device (I) and device (II).

with calcium cathodes reported in the literature [17,21,24–26].

In order to get further insight into the improved performance of the above PLEDs with LiF–Al based cathodes, we have measured the built-in potential (V_{bi}) of the devices by electroabsorption (EA). EA is a non-destructive and direct technique to measure the V_{bi} across the polymer layer and any shift in the cathodic barrier height upon changing contact material [5,11–13,23]. Fig 2 shows the electroabsorption spectrum and the absorption spectrum of a device (I). The absorption spectrum resembles that observed by Liess [15] and Campbell [12], however it rises faster at low energy than the spectrum observed by Yoon [13] The first maximum and zero transition of the electroabsorption spectra are at similar energy (±0.05 eV) as observed by other authors [12,13,15,23]. In contrast to the spectrum obtained by Campbell [12] the low energy positive wing is much more intense than the high energy negative wing. Such asymmetric features were also observed by other authors [13,15,23]. While the maximum and minimum are close to those of the second derivative of the absorption spectrum, they are situated at lower energy than the same features of the first derivative spectrum. On the other hand, in agreement with the first derivative spectrum the negative wing is much smaller than the positive wing.

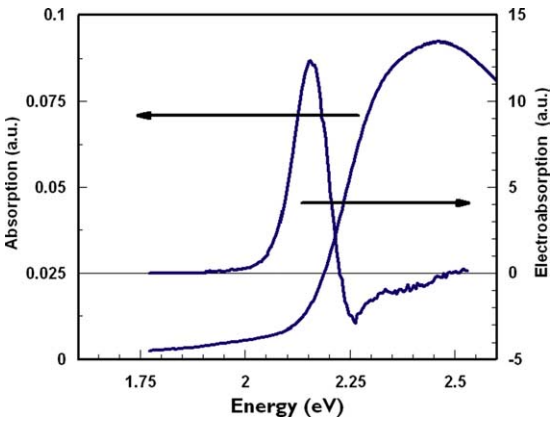

Fig. 2. Absorption and relative electroabsorption of an OLED at a bias of −3 V at 77 K.

Fig. 3 shows the dependence of the electroabsorption at 2.1 eV as a function of the applied bias voltage V_{bi}. A LiF:Al or LiF/Al cathode results in an increase of V_{bi} of approximately 0.5 V as compared to an Al cathode. An increased V_{bi} indicates a significant decrease of the potential barrier for electron injection at the polymer/cathode interface and hence an improved electron injection. As holes are majority carriers in devices with Al cathodes, an improved electron injection will lead to a more balanced density of electrons and holes and hence an improved η_{el} [21]. As expected following this line of thought replacing Al by Ag leads simultaneously to a decrease of V_{bi} and a decrease of η_{ext} (Table 2). We conclude that the improved electron injection resulting from a decrease of the effective work function of the cathode lays at the origin of the improved performance of PLEDs with LiF/Al cathodes [5,9]. Relating the V_{bi} and the dependence of V_{bi} upon the device configuration to the injection barrier and changes of the injection barrier is based on the assumption that the bulk of the PPV layer is free of space charge as is assumed also by several authors [5,12,13,27]. Strictly spoken such approach, which is also advocated for single crystals of organic

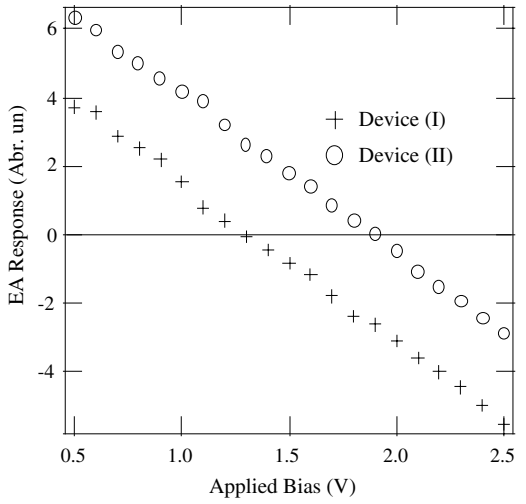

Fig. 3. Electroabsorption (ΔA) response of device (I) and device (II) at $h\nu$ = 2.10 eV as a function of applied bias at 77 K. V_{bi} corresponds to the bias at which the EA response intersects the zero axis.

molecules with orbital energies close to those of PPV [28], requires that the Fermi-level of the organic material is 0.8 V above or below that of the anode and the cathode [29,30]. Such will be the case for undoped PPV where the Fermi-level will be midway between the HOMO and the LUMO. In this case the electric field over the bulk of the semiconductor, where the largest part of the electroabsorption occurs will be the same everywhere. Even if the Fermi-level of PPV is lowered to 5.2 eV [5,12,27,31,32] a solution of the Poisson–Boltzmann problem [29,30] shows that unless a large concentration of dopants is assumed [32] this will only lead to deviations from a constant field close to the anode. Hence it will only lead to minor changes of the overall electroabsorption signal. It should be reported that sometimes [13] the dependence of V_{bi} upon the electrode cannot be explained in the framework of a nearly charge free polymer bulk. In this case there must be significant doping of the polymer [32].

We then examined the dependence of device efficiency upon the thickness of the LiF layer in LiF/Al cathodes. The results of the average values of maximum efficiency (η_{el}) and built-in voltage V_{bi} of devices with the different LiF thicknesses are shown in Table 1. The efficiency is almost independent of LiF thickness from 0.6 nm ($\eta_{el} = 2.0 \pm 0.2\%$) up to 4 nm ($\eta_{el} = 1.8 \pm 0.2\%$). However, η_{el} starts to drop from 4 nm to 8 nm ($\eta_{el} = 0.60 \pm 0.06\%$). We wish to emphasize that the change of η_{el} is in clear correspondence with the change of V_{bi}. The efficiency-LiF thickness relationship reported in this work is similar to reports on MEH-PPV based device with LiF/Al cathodes [8,9]. It differs with reports from Brown et al. [5], where PFO is used as the active polymer or from Jabbour et al., where the current, luminance and quantum yield increased with increasing thickness of the LiF layer deposited on an electron transport layer [22]. We attribute this difference to different types of emissive materials used in their devices and different preparations of the PLEDs.

In a further set of experiments, we varied the metal in LiF/metal cathodes to verify to what extent the covering metal plays a role. We choose Mg, a more chemically active metal than Al, and Ag, an inert metal for comparison. Devices with bare Mg and Ag as cathodes have η_{el} of 0.63%, 0.060% respectively. The η_{el} of the device with LiF(0.6 nm)/Mg and LiF(0.6 nm)/Ag cathodes are 1.7% and 0.00070%, respectively. We conclude that apparently, the chemical reactivity or work function of the covering metals does play a role. The smaller relative increase of efficiency upon inserting a LiF layer below a Mg electrode compared to the insertion below an Al electrode corresponds to results obtained for other PLEDs [27] and low molecular weight OLEDs [22].

The question arises whether Al plays an active role in LiF/Al cathode. To elucidate this point, we have fabricated devices with other fluoride cathode configurations. Namely, (1) cathodes consisting of a 2 nm thick layer of co-deposited LiF and Al composite layer, topped by another 50 nm of Al as protecting layer, and (2) cathodes composed of ultra-thin films of LiF(0.6 nm)/Al(1 nm) or LiF:Al (2 nm) covered by 100 nm Ag. The average values of maximum efficiency (η_{el}) and built-in voltage V_{bi} of devices with the above cathodes, as well as Ag and LiF/Ag

Table 1
Average values of maximum efficiency (η_{el}) and built-in voltage of devices based on LiF/Al cathodes with the different LiF thicknesses

LiF thickness (nm)	η_{el}	V_{bi} (V)
0	0.22 ± 0.02%	1.35 ± 0.050
0.6	2.0 ± 0.2%	1.85 ± 0.070
1.0	2.0 ± 0.2%	1.86 ± 0.10
2.0	1.9 ± 0.2%	1.80 ± 0.070
4.0	1.8 ± 0.2%	1.75 ± 0.070
6.0	1.5 ± 0.1%	1.69 ± 0.10
8.0	0.60 ± 0.06%	1.50 ± 0.10

Table 2
Average values of maximum efficiency (η_{el}) and built-in voltage V_{bi} of devices with the different cathodes

Cathodes	η_{el}	V_{bi} (V)
Al	0.22 ± 0.02%	1.35 ± 0.05
LiF(0.6 nm)/Al	2.0 ± 0.2%	1.85 ± 0.07
LiF:Al(50 nm)/Al	1.8 ± 0.2%	1.82 ± 0.07
Ag	0.060 ± 0.06%	0.75 ± 0.10
LiF(0.6 nm)/Ag	0.00070 ± 0.0001%	0.78 ± 0.10
LiF(0.6 nm)/Al(1 nm) Ag	1.9 ± 0.2%	1.80 ± 0.07
LiF:Al (2 nm)/Ag	1.8 ± 0.2%	1.82 ± 0.07

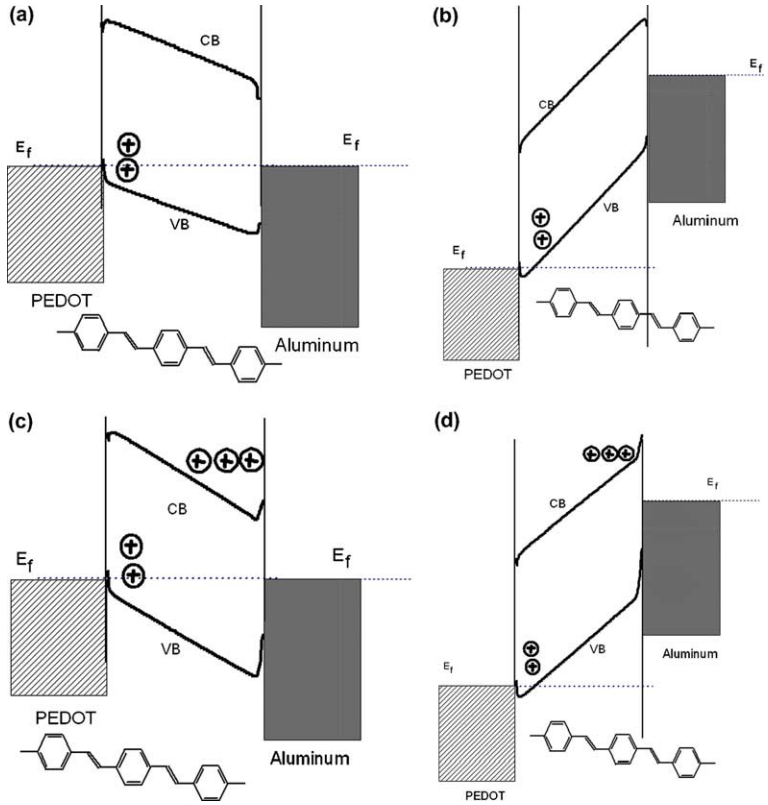

Fig. 4. Proposed energy-level diagram of the organic film without (a, b) and with LiF-incorporation (c, d). The positions of the highest occupied (labeled as VB), the lowest unoccupied orbital (labeled as CB) and the Fermi levels of the electrodes are shown respectively. While (a) and (c) correspond to equilibrium (no applied bias), (b) and (d) correspond to an applied bias of −3.3 V. The mismatch between the aluminum Fermi-level and the conduction band is 1.3 eV, while the energy difference between the cathode and the anode (PEDOT) is 1.0 eV. The band gap amounts to 2.4 eV.

cathodes are summarized in Table 2. All these LiF-modified devices show, in agreement to earlier results [9] comparable efficiency to device (II), which is also in correspondence with the almost identical values of the measured built-in voltage. It is interesting to notice that the value of η_{el} of the device with LiF(0.6 nm)/Ag cathode drops to two orders of magnitude less than that of device with a bare Ag cathode, while the V_{bi} remains almost the same in these two devices. This indicates that LiF remains as an insulator in the interface between the polymer and Ag and hinders the electron injection while not changing the band structure of the interface. By inserting ultra-thin films of LiF:Al or LiF between the Al-electrode and the polymer film this decrease of the current is not observed, either because LiF no longer behaves as an insulator or because the decreased electron transmission is overruled by other phenomena. This was also suggested by XPS spectra of Alq_3 covered by LiF and an Al layer with increasing thickness [4].

In order to discuss the role of LiF one has first to consider the details of profile of the energy levels and the charge injection process. In the absence of LiF and an externally applied field the profile of the energy levels taking into account the electrostatic potential is given in Fig. 4(a) and with more details for the interface where the electron injection occurs in Fig. 5(a). The energy levels calculated by solving the Poisson–Boltzmann equation in the absence of an externally applied field, take into account both the image potential [36] and

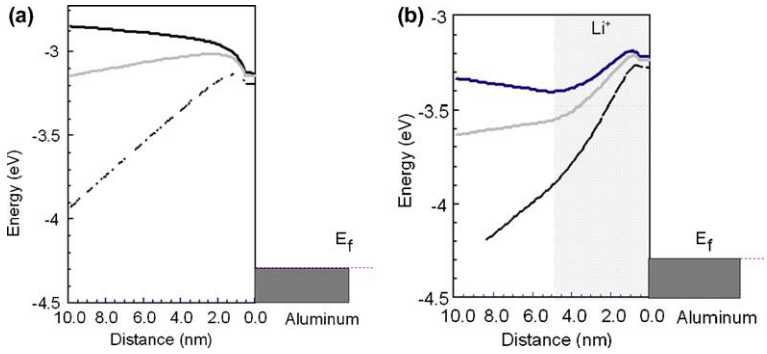

Fig. 5. Proposed energy-level diagram of the lowest unoccupied orbital in the organic film in the cathode region without (a) and with LiF-incorporation (b). —, — and ---- correspond to no bias, a bias of −3.3 V and a bias of −10.9 V of the aluminum electrode. The mismatch between the aluminium Fermi-level and the conduction band of the solid is 1.3 eV.

the space charges due to injected charge carriers [29,30,33–36] assuming a valence and conduction band at −5.4 V [12] and −3.0 V [12], and a Fermi energy for PEDOT and Al at respectively −5.3 [37] and −4.3 eV [12]. Under those conditions where no net current flow occurs, the electric field is mainly over the bulk of the sample. This situation corresponds to a difference of the electrostatic potential of 1.0 V, which is close to the opposite of the bias applied to the aluminum electrode (−1.35 V) necessary to eliminate the electroabsorption. When a net potential of −3.3 V is applied at the aluminum electrode (corresponding to a field of 2.4×10^5 V cm^{-1} in the bulk of the sample) the energy levels are in a first approximation (a superposition of the applied potential on the built-in potential) given by the energy diagramma in Figs. 4(b) and 5(a). As the barrier for electron injection at the level of Fermi-potential of aluminum is still more than 50 nm wide, injection is still largely a temperature assisted hopping process [33–40]. Under those conditions electron injection can be considered as a primary injection step followed by an escape over the image charge barrier in competition with recombination with empty energy levels above the Fermi-level of the metal [39]. Increasing the applied potential at the aluminum electrode to −10.9 V increases the field in the bulk of the sample to 9.4×10^5 V cm^{-1} and reduces the width of the energy barrier to about 10 nm. Under those conditions. the image charge barrier experienced by the injected charge carriers becomes so low and thin that all injected charges will escape and contribute to the current [39], however the primary injection step remains a thermally assisted process.

In this framework one could describe the dependence of the electron current on the barrier $\Delta\Phi$ between the energy of the LUMO and the Fermi-energy of the aluminum electrode in a very crude way by $\exp(-\Delta\Phi/kT)$. In this case the electron current should increase by a factor of 3×10^8 when the LiF layer is applied, as this barrier is reduced by 0.5 eV. This is clearly not observed. In the absence of LiF the electron current is at least 0.2% of the hole current at the applied bias voltage where η_{ext} is maximal, as η_{ext} amounts under those conditions to 0.2%. With LiF the total current has increased one order of magnitude, hence the electron current is now ten times the hole current (assuming an LiF layer at the cathode does not influence the hole current). Hence the whole current has increased at maximum by a factor 5000 (and probably much less). This is no surprise as the naïve dependence of the hole current on the Schottky barrier does clearly not correspond to reality at the complex interface between an organic charge transport material and a metal [36,39]. We should also remark that the increase of η_{ext} is even more modest than that of the electron current. η_{ext} depends upon more factors than just the balance between the electron and the hole current, furthermore as soon as this balance is reached any further increase of the electron current will decrease rather

than increase η_{ext} (although it can still increase the luminance).

In this framework we will now proceed with a critical review of the mechanisms that have been proposed to explain the role of LiF in the cathode of PLEDs, and relate them to our set of experiments on the role of LiF on the injection recombination and escape processes.

Tunneling through an insulating LiF layer over which a voltage drop is created has been proposed earlier as the mechanism for the injection enhancement [3]. Such insulating layer will at the same time reduce the back flow current [38–43] and increase the escape rate of the injected electron over the image charge barrier by increasing the distance between the starting position of the thermally assisted electron hopping and the electrode. The latter effect was observed upon covering anthracene crystals with insulating Langmuir Blodgett films [43]. On the other hand for electric fields up to $\approx 10^6$ V cm^{-1} the initial electron injection will become more endergonic and require tunneling over a larger distance in the presence of LiF barrier. Hence, such a theory predicts a strong dependence on the thickness of the LiF layer, which is contradicted by the result of Table 1. Furthermore this model cannot explain the change of the built-in field observed by electroabsorption (Table 1) or why an LiF layer causes no change in η_{ext} for an Ag cathode (Table 2). The most effective argument against this model is however that a ''mixed'' LiF:Al electrode yields the same results as a two layer system LiF/Al.

Other authors [9,41,44] propose that polarization of the LiF layer occurs at the interface under the influence of metal, which leads to a reduction of the effective work function. A different adsorption behaviour of LiF on aluminium and silver could explain why the LiF layer has a different effect upon both electrodes. Although such model can also explain the change of the built-in field observed by electroabsorption, it is not clear why or how LiF molecules could align to produce a bulk dipole moment as in case of self-assembling layers [45,46] unless they adsorb preferentially by the fluoride ion. Furthermore, in our experiment with composite cathodes, the LiF content is very small and it is hard to believe that LiF will form a separate layer that can be polarized. Moreover, such polarization effect would reach its maximum with a monolayer coverage, and drop rapidly with increasing layer thickness, which also contradicts our results as well as those of other authors [8,9].

Greczynski et al. [10] proposed that the main role of the LiF interfacial layer is to protect the polymer from damage during Al deposition. This theory, again, is compromised by our experiments with LiF:Al composite cathodes, as during the evaporation of the composite cathode the polymer remains in direct contact with the Al vapor and is not be protected by the LiF. Such model can again not explain the influence of LiF on the electroabsorption.

As an alternative method one could consider the formation of mixed Li–Al alloy which will be characterized by a lower work function [47–49]. Here we should remark that it was observed that deposition of a monolayer of alkali atoms on noble metals reduced the work function significantly even for a coverage below 10% of a monolayer [50,51]. Further increasing the coverage only introduced very small changes of the electrode work function. Such model can explain the observed effects of a LiF layer and of changes of the thickness of the LiF layer (Table 1) on the injection efficiency and the build-in bias. It furthermore explains why the same effects can also be observed with a LiF:Al alloy and why no effect is observed with an Ag electrode (Table 2). However to the extent this formation of an alloy requires the occurrence of the reaction $Al + 3LiF \rightarrow AlF_3 + 3Li$, it is problematic from a thermodynamic point of view [52]. Although the reduction of LiF by Al is thermodynamically highly unfavorable in a bulk phase, the presence of less stable LiF-clusters at the surface as well as the possibility to reduce the polymer close to the interface could change this thermodynamical aspect [4,52]. It is however questionable if the latter aspects would be sufficient to permit the reaction $Al + 3LiF \rightarrow AlF_3 + 3Li$.

Another approach resides in the diffusion of Li^+-ions, obtained by dissociation of LiF into the polymer. Those ions will build a space charge. In the next example we will try to evaluate what charge density and thickness of the space charge

layer built by those Li^+-ions is necessary to explain the experimental results. For e.g. a 5 nm space charge layer with a density (ρ) of 6×10^{18} cm^{-3} we would get the potential profile of Fig. 4(c) in the absence of an applied field. Comparing Fig. 4(a) and (c) shows that this space charge layer increases the built-in field over the bulk of the 110 nm polymer layer, which requires a larger negative bias on the aluminum electrode to get field free conditions in the bulk of the polymer layer. This corresponds to our experimental observations. As we have no direct information on the concentration profile of the Li^+-ions we must realize that a thinner space charge layer with a higher Li^+-ion concentration (or thicker space charge with a lower Li^+-ion concentration) will lead to an identical change of the built-in bias. Actually if we assume a rectangular space charge with thickness δ, all combinations of δ and ρ yielding the same value for $\delta^2\rho/2$ will yield the same change in V_{bi}. The only limits are that when δ gets too small the space charge density ρ and the total space charge $\rho\delta$ gets too large. On the other hand if ρ gets too small, δ gets very large and the injection barrier will remain too broad. Superimposing (for the case of Fig. 4(c)) an applied field of 2.4×10^5 V cm^{-1}, due an external bias, on the internal field yields the energy levels depicted in Figs. 4(d) and 5(b). Fig. 5(b) shows that the field of the space charge nearly levels the energy barrier due to the image charge. Furthermore for an electron in an energy level 0.9 eV above the Fermi-level the energy the barrier is less than 2 nm wide and 0.2 eV high allowing for an efficient combination of thermal assisted hopping and tunneling. At 9.4×10^5 V cm^{-1} the energy barrier has a width of less than 10 nm at the Fermi-level of aluminum and a height below 1.0 eV. This will allow for an efficient combination of thermal excitation to empty levels above the Fermi level and tunneling through the residual barrier. Hence the space charge of Li^+-ions will lead to much higher injection rate at the Al electrode. The space charge layer of 5 nm with 6×10^{18} Li^+-ions cm^{-3} corresponds to 3×10^{12} ions cm^{-2}, which is less than 0.5% of a monolayer. As only a tiny fraction of the deposited LiF (as separate layer or mixed with Al) is necessary to build this space charge layer it is no surprise that the way the LiF is added (mixed with Al or as a separate layer) or the thickness of the LiF layer have only a marginal influence on the properties of the device. Due the potential difference over this space charge layer the minimum of the LUMO energy (Figs. 4(c) and 5(b)) will get closer to the Fermi-level of the aluminum electrode. This will at equilibrium lead to a higher concentration of injected electrons in molecules close to the bottom of the potential well formed by combination of the intrinsic bias, the image charge and the space charge. Hence considering the charge carriers, the Li-ions lead to a (modest) n-doping of the organic layer close to the Al-electrode. From a purely formal point of view the interface resembles that between an organic layer with a thin modestly n-doped layer close to the surface and a metal electrode.

The n-doping of the organic layer close to the cathode we also find back in the model proposed by Mason et al. [4] and Piromreun et al. [8]. Based on the similarity of XPS spectra of Alq_3/LiF/Al and Alq_3/Li/Al multilayers they suggest that electrons are injected into Alq_3 upon deposition of Al on LiF leading to the formation of Alq_3-radical anion. Whether this process requires the intermediate formation of Li-atoms is highly uncertain. An argument in favor of diffusion of Li atoms resides in the fact that co-evaporating of Alq_3 and Li followed by deposition of an Al-electrode leads to similar results as consecutive deposition of a LiF layer and an Al-electrode on an Alq_3 layer [53,54]. However, as long as the conduction band of the organic layer is above that of the electrode, Alq_3^- anions formed by Li-atoms possibly diffusing in the organic will rapidly yield their electrons to the electrode until the electric potential difference over the space charge layer created by the remaining Li^+-ions matches the energy difference between the Fermi level of the electrode and the LUMO of Alq_3.

Whether the formation of Li atoms and their diffusion into the OC1C10 layer is followed by dissociation and equilibration of the electrons between the Al-electrode and the polymer or whether the diffusion of Li^+-ions and the formation of a space charge is followed by a redistribution of the electrons in this potential profile, an identical ion-and potential profile will be obtained.

The equilibration of the electrons between OC1C10 and the bulk electrode explains also why, as observed by us and other authors [53], the effect of the LiF layer depends on the nature of the underlying electrode (Al versus Ag). Compared to models involving the formation and diffusion of Li-atoms the diffusion of Li^+-ions does however not requite the thermodynamically unlikely reduction of Li^+-ions by aluminium.

Recent reports of secondary ion mass spectroscopy (SIMS) depth profile analysis reveals that the evaporation of Al on LiF leads to a spatial separation of Li and F induced by a chemical reaction of Al with LiF, where Li diffuses into the underlying organic layer while F is located mainly near the Al cathode [52]. The model proposed here, is not in contradiction with the SIMS experiments of Van Gennip et al. [55]. As only dissociation of a minor part of a monolayer of LiF is necessary there will still be an intense SIMS signal of LiF while only a very limited amount (if any) of AlF_3 will be formed.

4. Conclusions

We demonstrated that LiF/Al bilayers and LiF:Al composite layers facilitate efficient electron injection in PLEDs. The built-in potential in devices with these cathodes was found to be increased by 0.5 V as compared with Al. Our findings backs up the evidence for the hypothesis that evaporation of Al onto LiF produces a space charge close to the cathode/polymer interface due to doping with Li^+-ions. This space charge leads to modest n-doping, and a shift of the built-in potential in the same direction as indicated by the electro-adsorption experiments and decreases (height and width) barrier for electron injection. While compatible with the analytical and (opto)-electrical data on OLEDS or model systems incorporating LiF the present approach does not involve the thermodynamical unfavorable reduction of LiF by aluminum.

Acknowledgements

The authors are grateful to Professor P.W.M. Blom (University of Groningen) for discussion concerning his published results on OC1C10 based PLEDs with Ca cathode. We also thank Professor W.R. Salaneck (Linköping University) for technical discussions concerning UPS and XPS study on the interface of LiF and PFO. We thank Professor D. Vanderzande and Dr. L. Lusten (Limburgs Universitair Centrum) for providing OC1C10. The authors gratefully acknowledge the continuing support from Federal Science Policy (Belgium) through the grants IAP-IV-11 and IAP V-3, the F.W.O. Vlaanderen, the Nationale Loterij, the research Council of the K.U. Leuven through GOA 1996 and GOA 2001/2 and the European Union through COST D14.

References

[1] R.H. Friend, R.W. Gymer, A.B. Holmes, J.H. Burroughes, R.N. Marks, C. Taliani, D.D.C. Bradley, D.A. Dos Santos, J.L. Brédas, M. Lögdlund, W.R. Salaneck, Nature 397 (1999) 121.
[2] Y. Cao, G.Yu.I.D. Parker, A.J. Heeger, J. Appl. Phys. 88 (2000) 3618.
[3] L.S. Hung, C.W. Tang, M.G. Mason, Appl. Phys. Lett. 70 (1997) 13.
[4] M.G. Mason, C.W. Tang, L.S. Huang, P. Raychaudhuri, J. Madathil, L. Yan, Q.T. Le, Y. Cao, S.-T. Lee, L.S. Liao, L.F. Cheng, W.R. Salaneck, D.A. dos Santos, J.L. Brédas, J. Appl. Phys. 89 (2001) 2756.
[5] T.M. Brown, R.H. Friend, S. Millard, D.J. Lacey, J.H. Burroughes, F. Cacialli, Appl. Phys. Lett. 77 (2000) 3096.
[6] L.C. Palilis, D.G. Lidzey, M. Redecker, D.D.C. Bradley, M. Inbasekaran, E.P. Woo, W.W. Wu, Synth. Met. 111–112 (2000) 163.
[7] N.K. Patel, S. Cina, J.H. Burroughes, IEEE J. Selected Topics Quantum Electron. 8 (2002) 1.
[8] P. Piromreun, H. Oh, Y. Shen, G.G. Malliaras, J.C. Scott, P.J. Brock, Appl. Phys. Lett. 77 (2000) 2403.
[9] X. Yang, Y. Mo, W. Yang, G. Yu, Y. Cao, Appl. Phys. Lett. 79 (2001) 563.
[10] G. Greczynski, M. Fatlman, W.R. Salaneck, J. Chem. Phys. 113 (2000) 2407.
[11] P.W.M. Blom, H.C.F. Martens, H.E.M. Schoo, M.C.J.M. Vissenberg, J.N. Huiberts, Synth. Met. 122 (2001) 95.
[12] I.H. Campbell, T.W. Hagler, D.L. Smith, J. Ferraris, Phys. Rev. Lett. 76 (1996) 1900.
[13] J. Yoon, J.-J. Koo, T.-W. Lee, O.-O. Park, Appl. Phys. Lett. 76 (2000) 2152.
[14] S.A. Jeglinsky, Z.V. Vardenny, Y. Ding, T. Barton, Mol. Cryst., Liquid Cryst. 256 (1994) 87–96.
[15] M. Liess, S. Jeglinski, Z.V. Vardenny, M. Ozaki, K. Yoshino, Y. Ding, T. Barton, Phys. Rev. B 56 (1997) 15712.

[16] Y.D. Jin, H.Z. Chen, P.L. Heremans, K. Aleksandrzak, H.J. Geise, G. Borghs, M. Van der Auweraer, Synth. Met. 127 (2002) 155.
[17] L. Lutsen, P. Adriaensens, H. Becker, A.J. Van Breemen, D. Vanderzande, J. Gelan, Macromolecules 32 (1999) 6517.
[18] P.W.M. Blom, private communication.
[19] N.C. Greenham, R.H. Friend, D.D.C. Bradley, Adv. Mater. 6 (1994) 491.
[20] S. Sebastian, G. Weiser, H. Bässler, Chem. Phys. 61 (1981) 125.
[21] P.W.M. Blom, M.J.M. De Jong, Philips J. Res. 51 (1998) 479.
[22] G.E. Jabbour, Y. Kawabe, S.E. Shaheen, J.F. Wang, M.M. Morrell, B. Kippelen, N. Peyghambarian, Appl. Phys. Lett. 71 (1997) 1762.
[23] S.A. Whitelegg, C. Giebeler, A.J. Campbell, S.J. Martin, P.A. Lane, D.D.C. Bradley, G. Webster, P.L. Burn, Synth. Met. 111 (2000) 241.
[24] I.D. Parker, Y. Cao, Y. Yang, J. Appl. Phys. 85 (1999) 2441.
[25] W. Bijnens, Ph.D. Thesis, Limburgs Universitair Centrum, 1998.
[26] Y. Cao, I.D. Parker, G. Yu, C. Zhang, A.J. Heeger, Nature 397 (1999) 414.
[27] T.C. Brown, R.H. Friend, I.S. Millard, D.J. Lacey, J.H. Burroughes, F. Cacialli, Appl. Phys. Lett 79 (2001) 174.
[28] E. Silinsh, Organic Molecular Crystals, Springer, Belin, 1980, pp. 280–285.
[29] J.S. Bonham, D.H. Jarvis, Aust. J. Chem. 30 (1977) 705.
[30] J.S. Bonham, Aust. J. Chem. 31 (1978) 1661–2103.
[31] C. Ganzori, M. Fujihira, Jpn. J. Appl. Phys 38 (1999) L-1348.
[32] S. Karg, M. Mier, W. Riess, J. Appl. Phys. 82 (1997) 1951.
[33] D.F. Blossey, Phys. Rev. B 11 (1974) 5183.
[34] A. Prock, K.N. Das, P. Melman, J. Chem. Phys. 79 (1983) 4069.
[35] Y. Gartstein, E.M. Conwell, Chem. Phys. Lett. 255 (1996) 93.
[36] V.I. Arkhipov, E.V. Emilianova, Y.H. Tak, H. Bässler, J. Appl. Phys. 84 (1998) 848.
[37] T.M. Brown, J.S. Kim, R.H. Friend, R. Daik, W.J. Feast, Appl. Phys. Lett. 75 (1999) 1679.
[38] J. Campbell Scott, G.G. Malliaras, Chem. Phys. Lett. 299 (1999) 115.
[39] V.I. Arkhipov, U. Wolf, H. Bässler, Phys. Rev. B 59 (1999) 7514.
[40] J. Rommens, M. Van der Auweraer, F.C. De Schryver, J. Phys. Chem. B 101 (1997) 3081.
[41] B. Masennelli, E. Tutis, M.N. Bussac, L. Zuppiroli, Synth. Met. 122 (2001) 141.
[42] M. Stöszel, J. Staudigel, F. Steuber, J. Blässing, J. Simmerer, A. Winnacker, Appl. Phys. Lett. 76 (2000) 115.
[43] M. Van der Auweraer, G. Biesmans, B. Verschuere, F.C. De Schryver, F. Willig, Langmuir 3 (1987) 992.
[44] G. Greczynski, M. Fahlman, W.R. Salaneck, Appl. Surf. Sci. 166 (2001) 380.
[45] I.H. Campbell, J.D. Kress, R.L. Marti, D.L. Smith, Appl. Phys. Lett 71 (1997) 3528.
[46] L.S. Hung, R.Q. Zhang, P. He, G. Mason, J. Phys. D: Appl. Phys. 35 (2002) 103.
[47] S.E. Shaheen, G.E. Jabbour, M.M. Morrell, Y. Kawabe, B. Kipplen, N. Peyghambarian, J. Appl. Phys. 84 (1998) 2324.
[48] J. Kido, K. Nagai, Y. Okamoto, IEEE Trans. Electron. Dev. 40 (1993) 1342.
[49] S. Naka, M. Tamekawa, T. Terashita, H. Okada, H. Anada, H. Onnagawa, Synth. Met. 91 (1997) 129.
[50] A. Neumann, S.L.M. Schroeder, K. Christmann, Phys. Rev. B 15 (1995) 17007.
[51] W. Ning, C. Kailai, W. Dinsheng, Phys. Rev. Lett. 56 (1986) 2759.
[52] H. Heil, J. Steiger, S. Karg, M. Gastel, H. Ortner, H. von Seggen, M. Stößel, J. Appl. Phys. 89 (2001) 420.
[53] J. Kido, T. Matsumoto, Appl. Phys. Lett. 73 (1998) 2866.
[54] L.S. Hung, C.W. Tang, M.G. Mason, P. Raychaudhuri, J. Madathil, Appl. Phys. Lett. 78 (2001) 544.
[55] W.J.H. van Gennip, J.K.J. van Duren, P.C. Thüne, R.A.J. Janssen, J.W. Niemantsverdriet, J. Chem. Phys. 117 (2002) 5031.